View metadata, citation and similar papers at core.ac.uk
brought to you by CORE
provided by DSpace@MIT

# First-principles study of point defects in $LaAlO_3$

J.X. ZHENG,[1] G. CEDER,[1,2] W.K. CHIM,[1,3] and W.K. CHOI[1,3]
[1] Singapore-MIT Alliance, 4 Engineering Drive 3, Singapore 117576
[2] Department of Materials Science and Engineering, Massachusetts Institute of Technology, 77 Massachusetts Avenue, Cambridge, MA 02139-66307, USA
[3] Department of Electrical & Computer Engineering, National University of Singapore, 4 Engineering Drive 3, Singapore 117576

***Abstract*—In this study, the native point defects including oxygen vacancy and interstitial, metal (La, Al) vacancy and interstitial, and metal antisite in perovskite LAO are studied. Defect formation energies are studied as a function of the external chemical potentials and Fermi level. The stable defects are identified under different external chemical potentials and Fermi levels. The effect of image charge corrections is also investigated. Finally, based on results in this study, optimal growth conditions can be proposed to achieve better defect engineering for LAO gate dielectrics.**

*Index Terms* —**high-k gate dielectrics, first-principles calculation, point defect.**

## I. Introduction

As the feature sizes of semiconductor devices continue to shrink, searching for appropriate high dielectric constant (high-k) gate dielectrics as a replacement of silicon dioxide ($SiO_2$) remains a very challenging task. According to the 2005 International Roadmap for Semiconductors [1], a progression from hafnium-based dielectrics to Group III and/or rare earth (RE) oxides to ternary oxides may be required. Currently for a high-k gate dielectric grown on top of a silicon substrate, an unintentional interfacial $SiO_2$ layer is required to preserve the interface quality. Unfortunately this interfacial layer limits the lowest effective oxide thickness. An epitaxial gate dielectric can potentially eliminate the interfacial layer and result in a sharp interface with the silicon substrate.

Lanthanum aluminum oxide, or $LaAlO_3$ (LAO), is a promising candidate for epitaxial oxides. It has a dielectric constant of 24, a large band gap of 5.5 eV [2], a reasonable conduction band offset with silicon [3], and it is thermodynamically stable in contact with silicon.

## II. Computational Methodology

Our calculations are based on density functional theory (DFT) in the generalized gradient approximation (GGA) with the functional of Perdew, Burke, and Ernzerhof (PBE) for the exchange correlation potential, as implemented in the VASP program (Vienna *ab-initio* simulation package) [4,5]. Projector augmented wave (PAW) pseudopotentials are used to model the interaction of the valence electrons with the core electrons [6,7]. The pseudopotential for La is generated in the $5s^2 5p^6 5d^1 6s^2$ configuration and that for Al is in the $3s^2 3p^1$ configuration. The configuration $2s^2 2p^4$ is used for the generation of the pseudopotential of oxygen.

The formation energy of a point defect depends on the chemical potentials as well as on the Fermi level if the point defect is charged. The ranges of chemical potentials $\mu_{La}, \mu_{Al}, \mu_O$ are bound by (i) the values that prevent the formation of pure metals and $O_2$ gas:

$$\mu_{La} \le \mu_{La}^o; \qquad \mu_{Al} \le \mu_{Al}^o; \qquad \mu_O \le \mu_O^o \tag{1}$$

(ii) the values that prevent the formation of binary oxides:

$$2(\mu_{La} - \mu_{La}^o) + 3(\mu_O - \mu_O^o) \le \Delta E_f^{La_2O_3} \tag{2}$$

$$2(\mu_{Al} - \mu_{Al}^o) + 3(\mu_O - \mu_O^o) \le \Delta E_f^{Al_2O_3} \tag{3}$$

and (iii) the values that maintain a stable LAO compound:

$$(\mu_{La} - \mu_{La}^o) + (\mu_{Al} - \mu_{Al}^o) + 3(\mu_O - \mu_O^o) = \Delta E_f^{LaAlO_3} \tag{4}$$

By substituting Eq. (4) in (3) and making some arrangement, we can get

$$2(\mu_{La} - \mu_{La}^o) + 3(\mu_O - \mu_O^o) \ge 2\Delta E_f^{LaAlO_3} - \Delta E_f^{Al_2O_3} \tag{5}$$

Now the ranges of atomic chemical potentials are completely defined by Eqs. (2) and (5) with $\mu_{La}$ and $\mu_O$. Thus we can plot the stability quadrangle in Fig. 1.

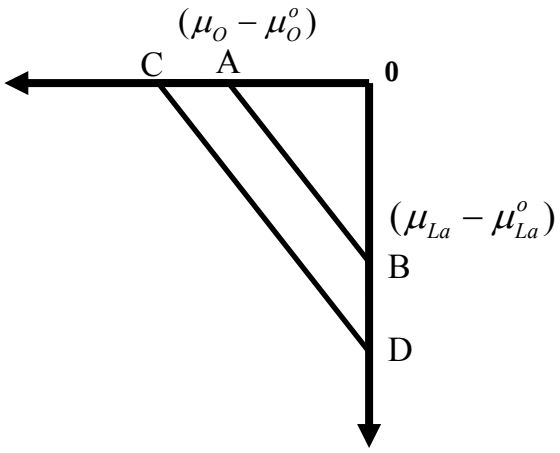


Fig. 1. The stability quadrangle for $LaAlO_3$ in the $\{\mu_{La}, \mu_O\}$ plane. The chemical potential ranges for $\mu_{La}$ and $\mu_O$ are defined with the region ABCD.

The formation energy ($E_f$) of forming a point defect α with charge q, [$\alpha^q$], in $MO_2$ (M = Hf, Zr) is computed as

$$E_f[\alpha^q] = E[\alpha^q] \pm \mu_X - E[bulk] + q(E_V + \Delta V + \varepsilon_F), \quad (6)$$

where $E[\alpha^q]$ is the total energy of the supercell containing the point defect, $\mu_X$ is the elemental chemical potential with a positive sign for vacancies and a negative sign for interstitial defects, $E$[bulk] is the total energy of the perfect supercell, $E_V$ is the valence band maximum (VBM) of the perfect supercell, and $\varepsilon_F$ is the Fermi level which is referenced to $E_V$. The shift of the VBM in a defect supercell, $\Delta V$, takes the change of the valence band maximum caused by the defect into account. It can be obtained using a macroscopic averaging technique,[39-40] by calculating the difference between the average electrostatic potential in a bulklike environment of the defect supercell and the average electrostatic potential in the perfect supercell.

The defect interaction between charged defects due to finite supercell size can introduce an error on the order of 0.1 eV, and this error may become larger for higher-charged defects. There is an ongoing debate on how to apply appropriate image charge corrections.[37,41-43] Although the Makov-Payne correction works well for atomic or molecular systems, it represents the upper limit of correction for solids as it is based on the assumption of localized defect charges and the neglect of screening from valence electrons. As a more accurate image charge correction scheme is still lacking, we will use the Makov-Payne scheme for the image charge correction. The typical problem of DFT with underestimating band gaps may also have implications for the energy of defects with filled states having conduction band character.

The thermodynamic transition between two charge states, $q_1$ and $q_2$, on the defect occurs for the Fermi level at which the formation energy of [$q_1$] is equal to that of [$q_2$]. It can be shown that the thermodynamic transition level $q_1/q_2$ is

$$\varepsilon_F[q_1/q_2] = \frac{1}{q_2 - q_1}\{E[q_1] - E[q_2] + q_1(E_V + \Delta V_1) - q_2(E_V + \Delta V_2)\}, \quad (7)$$

where $q_1$ and $q_2$ are respectively the initial and final charge states (including the signs), $\Delta V_1$ and $\Delta V_2$ are the VBM shift for the initial and final charge states, and $\varepsilon_F[q_1/q_2]$ is the Fermi energy level at which the transition from $q_1$ to $q_2$ takes place.

## III. Results

LAO is a 3-3 valence perovskite, which is different from $SrTiO_3$ (STO). This 3-3 valence makes LaO and $AlO_2$ layers polar. Thus LAO consists of alternating layers of positively charged $(LaO)^+$ and negatively charged $(AlO_2)^-$. This is different from STO where both layers are charge neutral.

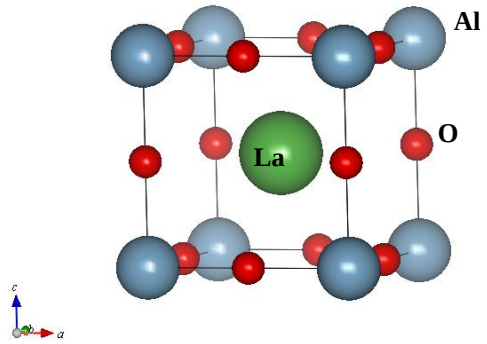


Fig. 2. The unit cell of $LaAlO_3$.

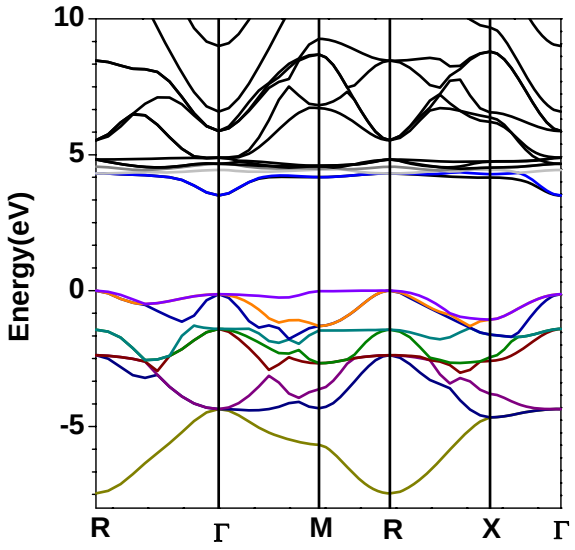


Fig. 3. Calculated band structure of bulk $LaAlO_3$. The energy 0 eV is set at the VBM at R.

For calculation of a unit cell of LAO, a Monkhorst-Pack 12x12x12 *k*-point grid is used for the Brillouin zone integration The calculated band gap of LAO is 3.6 eV, compared to experimental band gap of 5.5 eV. This underestimation is typical under DFT framework with GGA approximation.

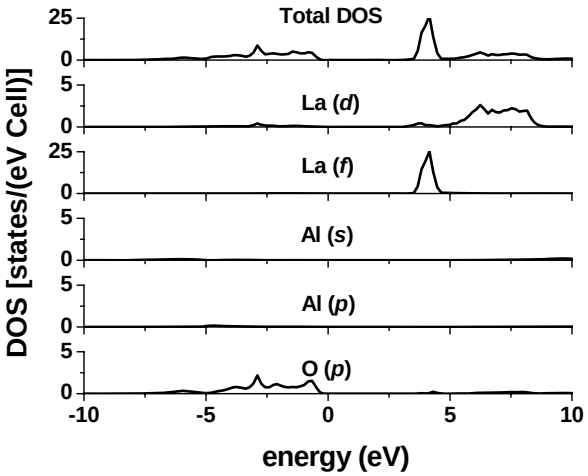


Fig. 4. Total density of states (DOS) and atomic-orbital resolved DOS.

The total and atomic-orbital resolved density of states (DOS) are shown in Fig. 3. The top of the valence band is formed by O 2*p* states, and the bottom of the conduction band is from La *f* states. It is not clear why La *f* states form the bottom of the conduction band as it is not reported elsewhere [8].

## REFERENCES

[1] International Technology Roadmap for Semiconductors, http://public.itrs.net/.
[2] S. G. Lim, S. Kriventsov, T. N. Jackson, J. H. Haeni, D. G. Schlom, A. M. Balbashov, R. Uecker, P. Reiche, J. L. Freeouf, and G. Lucovsky, J. Appl. Phys. **91**, 4500 (2002).
[3] L. F. Edge, D. G. Schlom, S. A. Chambers, E. Cicerrela, J. L. Freeouf, B. Hollander, and J. Schubert, Appl. Phys. Lett. **84**, 726 (2004).
[4] J. P. Perdew, K. Burke, and M. Ernzerhof, Phys. Rev. Lett. **77**, 3865 (1996).
[5] G. Kresse and J. Furthmüller, Phys. Rev. B **54**, 11169 (1996); G. Kresse and J. Furthmüller, Comput. Mat. Sci. **6**, 15, (1996).
[6] G. Kresse and D. Joubert, Phys. Rev. B **59**, 1758 (1999).
[7] P. E. Blöchl, Phys. Rev. B **50**, 17953 (1994).
[8] K. Xiong, J. Robertson, and S. J. Clark, Appl. Phys. Lett. **89**, 022907 (2006).